



EFFECTS OF THERMO DIFFUSION AND TRANSVERSE MAGNETIC FIELD ON HEAT TRANSFER OVER A STRETCHING CYLINDER UNDER CONVECTIVE BOUNDARY CONDITION

N.S.L.V. Narasimha Rao
Department of Mathematics
Acharya Nagarjuna University
Ongole, Andhra Pradesh -523001, India

K. Gangadhar
Department of Mathematics
Acharya Nagarjuna University
Ongole, Andhra Pradesh -523001, India

Abstract: A numerical behaviour for axisymmetric flow and heat transfer due to a stretching cylinder under the influence of a uniform magnetic field, thermo diffusion and convective condition is presented. The governing partial differential equations are rehabilitated into nonlinear, ordinary, and coupled differential equations and are solved with Keller-Box technique. The effects of key parameters such as magnetic parameter, curvature parameter, Prandtl number, Soret number and the local Biot number are explained by the graphs. The numerical outcomes are compared with the published data and are found to be in an excellent agreement.

Keywords: MHD, Thermo Diffusion, Heat Transfer, Convective Heating.

I. INTRODUCTION

Magneto-hydraulics (MHD) boundary layers through heat and mass transfer over flat surfaces are recognized in numerous engineering and geophysical applications such as cooling of nuclear reactors, geothermal reservoirs, thermal insulation, enhanced oil recovery and packed-bed catalytic reactors. In numerous chemical engineering processes like metallurgical and polymer extrusion processes absorb cooling of a molten liquid being stretched into a cooling method. The fluid mechanical properties of the last product depend primarily on the cooling liquid worn and the rate of stretching. A number of polymer liquids like polyethylene oxide and polyisobutylene solution have improved electromagnetic properties are normally worn as cooling liquid as their flow container be keeping up by outside magnetic fields in order to progress the eminence of the final product. Rahman et al. [1] observed the effects of joule heating and magneto-hydro dynamics mixed convection in an obstructed lid-driven square cavity. Olanrewaju et al. [2] studied the stagnation point flow of micro polar fluid over a vertical plate with thermal radiation and MHD. Gangadhar [3] investigated the effects of viscous dissipation and radiation on MHD boundary layer flow of heat and mass transfer through a porous vertical flat plate. Mohammed Ibrahim et al. [4] investigated on oscillatory flow of heat and mass transfer of MHD. Rawat et al. [5] studied the effects of MHD and Non Darcy porous medium on micro polar fluid over a non-linear stretching sheet and they concluded that on mounting the material parameter leads to a declining skin-friction coefficient and also couple stress.

It is well established fact that Fourier's law gives an expression relating to energy flux with temperature gradient. Fick's law shows the relation between the mass flux and concentration gradient. It also pointed out that energy flux can also be caused by composition pressure gradients. Dufour pointed out about the production of energy flux by composition gradient and hence in literature it was referred to the thermo-diffusion effect or the Dufour effect. Soret also observe that the temperature gradient creates the mass flux. Note that both these effects are have small order of

magnitudes when compared with the Fourier's or Fick's laws and usually neglected the effect of heat and mass transfer situations. Note that thermo-diffusion effect is very important for isotope separation and in mixture between the gases with very light molecular weight (H_2 , He) and of medium molecular weight (N_2 , air) [6] and in such situations thermo-diffusion effect cannot be ignored. Makinde and Olanrewaju [7] observed the Soret and Dufour effects in an unsteady mixed convection flow over a porous medium, plate moving through a binary mixture of chemically reacting fluid. Shehzad et al. [8] presented the analytical solution of Soret and Dufour effects on the stagnation point flow of Jeffery fluid under convective boundary conditions. Makinde [9] also studied the Soret and Dufour effects in MHD mixed convection flow over a vertical porous plate. Recently, Olanrewaju and Makinde [10] studied the effects of thermal diffusion in chemically reacting MHD boundary layer flow of heat and mass transfer through a vertical plate with suction/injection.

Many researchers recently studied recently on the boundary layer flow problems with a convective surface boundary condition have achieved to a great extent. This was first established by Aziz [11], who considered the thermal boundary layer flow over a flat plate in a uniform free stream with a convective surface boundary condition. This problem was extended by Bataller [12] by considering the both Blasius and Sakiadis flows under a convective surface boundary condition in the presence of thermal radiation. Gangadhar et al. [13] investigated the hydrodynamic effect on heat and mass transfer through a vertical plate with additional effects of convective boundary condition and chemical reaction. Ishak [14] find the similarity solutions for the steady laminar boundary layer flow with a convective boundary condition over a permeable plate. Makinde and Aziz [15] investigated numerically the effect of a convective boundary condition on the two dimensional boundary layer nanofluid fluid flows past a stretching sheet.

So far as we are aware, no attempt has ever been made to study the impact of magnetic field, thermo diffusion and

prescribed convective heating on axisymmetric boundary layer flow along a stretching cylinder. In this paper, the governing partial differential equations of the flow and temperature fields are reduced to ordinary differential equations, which are solved numerically by using Keller – Box method.

II. MATHEMATICAL FORMULATION

A study considered that the axisymmetric boundary layer flow of an incompressible viscous fluid over a circular stretching cylinder of radius a with a constant temperature T_∞ . The x -axis is measured along the tube, and the r -axis is calculated in the radial direction.

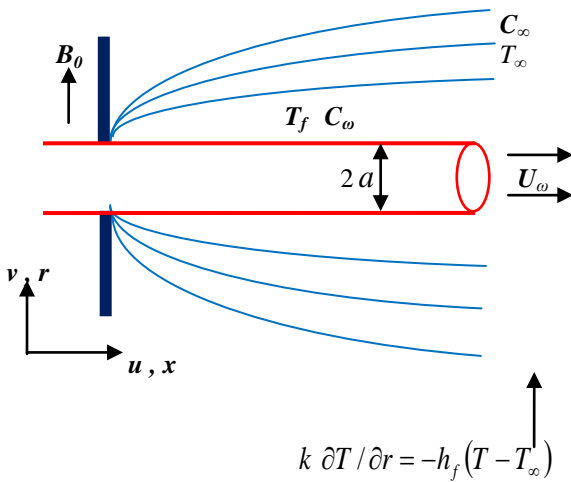


Figure 1: Diagram of the physical problem

A uniform magnetic field of strength B_0 is implicit to act in the radial direction, while the induced magnetic field is negligible, which can be justified for MHD flow at small magnetic Reynolds number [16]. Further, the cylinder is assumed to be axially stretched with velocity $U_\omega(x) = U_0(x/L)$, where U_0 is a constant and L is the characteristics length as shown in Fig. 1.

With these assumptions, the boundary layer equations govern the flow and heat transfer

$$\frac{\partial(ru)}{\partial x} + \frac{\partial(rv)}{\partial r} = 0 \tag{1}$$

$$u \frac{\partial u}{\partial x} + v \frac{\partial u}{\partial r} = \nu \left(\frac{\partial^2 u}{\partial r^2} + \frac{1}{r} \frac{\partial u}{\partial r} \right) - \frac{\sigma B_0^2}{\rho} u \tag{2}$$

$$u \frac{\partial T}{\partial x} + v \frac{\partial T}{\partial r} = \alpha \left(\frac{\partial^2 T}{\partial r^2} + \frac{1}{r} \frac{\partial T}{\partial r} \right) \tag{3}$$

$$u \frac{\partial C}{\partial x} + v \frac{\partial C}{\partial r} = D \left(\frac{\partial^2 C}{\partial r^2} + \frac{1}{r} \frac{\partial C}{\partial r} \right) + \bar{S} \left(\frac{\partial^2 T}{\partial r^2} + \frac{1}{r} \frac{\partial T}{\partial r} \right) \tag{4}$$

were u and v are the fluid velocity components along x -direction, r - directions respectively, ν is the kinematic viscosity, σ is electrical conductivity, B_0 is the transverse magnetic field, ρ is the fluid density, α is the thermal diffusivity, T is the fluid temperature in the boundary layer, \bar{S} is the thermo diffusion coefficient and C is the fluid concentration in the boundary layer.

The hydrodynamic boundary conditions of this problem are

$$u = U_\omega(x) = U_0 \left(\frac{x}{L} \right), v = 0 \text{ at } r = a \tag{5}$$

and $u \rightarrow 0$ as $r \rightarrow \infty$ (5)

The thermal and concentration boundary conditions are

$$k \frac{\partial T}{\partial r} = -h_f (T - T_\infty) \text{ at } r = a \text{ and } T \rightarrow T_\infty \text{ as } r \rightarrow \infty \tag{6}$$

$$C = C_\omega \text{ at } r = a \text{ and } C \rightarrow C_\infty \text{ as } r \rightarrow \infty \tag{7}$$

here subscript w corresponds to the wall condition; h_f is the convective heat transfer coefficient; T_f is the ambient fluid temperature; C_ω the ambient fluid concentration.

The continuity equation (1) is satisfied by introducing the stream function ψ such that

$$u = \frac{1}{r} \frac{\partial \psi}{\partial x} \text{ and } v = -\frac{1}{r} \frac{\partial \psi}{\partial r}$$

η and ψ can be defined Mukhopadhyay [16] as

$$\eta = \frac{r^2 - a^2}{2a} \left(\frac{U_\omega}{\nu x} \right)^{\frac{1}{2}}, \psi = (\nu x U_\omega)^{\frac{1}{2}} af(\eta), \frac{T - T_\infty}{T_f - T_\infty} = \theta(\eta), \frac{C - C_\infty}{C_w - C_\infty} = \psi(\eta) \tag{8}$$

Where f is the dimensionless stream function and η is the similarity variable. By defining η in this way, the boundary condition at $r = a$ is reduced to the boundary condition at $\eta = 0$, which is further suitable for numerical computations [17].

$$u = U_\omega f'(\eta), v = -\frac{a}{r} \left(\frac{\nu U_0}{L} \right)^{\frac{1}{2}} f(\eta) \tag{9}$$

Substituting (8)- (9) into (2)-(7), the governing equations and boundary conditions reduce to

$$(1 + 2\gamma\eta)f''' + 2\gamma f'' + ff'' - f'^2 - \frac{M}{1 + 2\gamma\eta} f' = 0 \tag{10}$$

$$(1 + 2\gamma\eta)\theta'' + 2\gamma\theta' + Pr(f\theta' - f'\theta) = 0 \tag{11}$$

$$(1 + 2\gamma\eta)\phi'' + 2\gamma\phi' + Sc(f\phi' - f'\phi) + SrSc(1 + 2\gamma\eta)\theta'' + 2SrSc\gamma\theta' = 0 \tag{12}$$

Subject to the boundary conditions

$$f = 0, f' = 1, \theta' = -Bi(1 - \theta), \phi = 1 \text{ at } \eta = 0 \tag{13}$$

$$f' \rightarrow 0, \theta \rightarrow 0, \phi \rightarrow 0 \text{ as } \eta \rightarrow \infty \tag{14}$$

Where $\gamma = \sqrt{\frac{\nu L}{U_0 a^2}}$ is the curvature parameter,

$M = \frac{\sigma B_0^2 L}{\rho U_0}$ is the magnetic parameter, $f_\omega = -V \sqrt{\frac{L}{\nu U_0}}$

is suction ($f_\omega > 0$) and injection ($f_\omega < 0$) parameter,

$Pr = \frac{\nu}{\alpha}$ is Prandtl number, $Sc = \frac{\nu}{D}$ is Schmidt number,

$Sr = \frac{\bar{S}(T_\omega - T_\infty)}{\nu(C_\omega - C_\infty)}$ is Soret number. Note that for a

cylinder $\gamma = 1$ and for a plate $\gamma = 0$. $M = 0$ (without magnetic field) and $f_\omega = 0$ (without suction/injection), the problem under consideration reduces to that considered by Ishak *et al.* [18] (with $\varepsilon = M = 0, n = 1$) and Liu [19] (with $Mn = 0, \beta = 1$) in those papers. For particular cases, the solutions of the present stretching cylinder model well competition with those accounted by Ishak *et al.* [18], and Liu [19] for stretching plate.

Quantities of physical interest for the phenomena we are studying the skin friction coefficient C_f and the local Nusselt number Nu_x . Physically, C_f represents the wall shear stress and Nu_x defines the heat transfer rate and these can be written as

$$C_f = \frac{2\tau_\omega}{\rho U_\omega^2}, \text{ and } Nu_x = \frac{xq_\omega}{k(T_f - T_\infty)} \quad (15)$$

here τ_ω is the skin friction and q_ω is heat flux from the cylinder which are given by

$$\tau_\omega = \mu \left(\frac{\partial u}{\partial r} \right)_{r=a}, \text{ and } q_\omega = -k \left(\frac{\partial T}{\partial r} \right)_{r=a} \quad (16)$$

Substituting (8) into (15)-(16), we get

$$\frac{1}{2} \sqrt{Re_x} C_f = f''(0) \text{ and } \frac{Nu_x}{\sqrt{Re_x}} = -\theta'(0) \quad (17)$$

Where $Re_x = \frac{U_\omega x}{\nu}$ is the local Reynolds number.

III. SOLUTION OF THE PROBLEM

Equations (10)-(12) are nonlinear, it is not possible to obtain the closed form solutions, as a result the equations through the boundary conditions (13) & (14) are solved numerically by means of a finite-difference scheme recognized as the Keller-box method. The major steps in the Keller-box method to obtain the numerical solutions are the following:

- Decrease the specified ODEs to a system of first order equations.
- Write down the condensed ODEs to finite differences.
- Linearized the algebraic equations by using Newton's method and write down them in vector form.
- Solve the linear system through the block tridiagonal elimination technique.

$$f_0(\eta) = f_\omega + 1 - e^{-\eta}, \quad p_0(\eta) = e^{-\eta}, \quad g_0(\eta) = \frac{Bi}{Bi + 1} e^{-\eta}$$

In this study, a consistent grid of size $\Delta\eta = 0.006$ is found to be convince the convergence and the solutions are obtained through an error of tolerance 10^{-5} in all cases. In our study, this gives regarding six decimal places perfect to the majority of the agreed quantities.

IV. RESULTS AND DISCUSSION

In this section we present solutions of equations (10)-(12) along with the boundary conditions (13) and (14) using the Keller – Box method iteration method. Tables 1 gives a

comparison between the present results and Butt and Ali [20], Fang *et al.* [21], Mukhopadhyay [22] and Maboob *et al.* [23] for the local skin-friction coefficient. There is a good agreement between the two sets of results with the Keller-Box method having up to seven decimal places. The velocity components for axial $f(\eta)$ and transverse $f'(\eta)$ are plotted in Fig. 2 for different values of the magnetic field parameter M for both cylinder and plate respectively. It is clear that the velocities decreases with increases in the magnetic parameter. Increasing magnetic interaction number M from purely hydrodynamic case $M = 0$ to higher values of M , gives rise to a strong deceleration in the flow. Presence of a magnetic field in an electrically conducting fluid introduces a Lorentz force which acts against the flow in the case that magnetic field is applied in the normal direction as considered in the present problem. The described type of resistive force tends to slow down the flow field. For all situations, the velocity vanishes far from the surface of the cylinder. Higher the value of M , the more prominent is the reduction in hydrodynamic boundary layer thickness. The Prandtl number gives no effect to the velocity profile can be seen from Eq. (10).

Figures 3 and 4 illustrate the dimensionless temperature and concentration profiles for various values of magnetic parameter M for both cylinder and plate. Generally, the temperature and concentration is the maximum at the plate surface but decreases exponentially to zero far away from the plate surface satisfying the free stream conditions. The magnetic field has profound effects on the temperature and concentration profiles. The effect of transverse magnetic field M is to enhance the temperature and concentration profiles since M reduces the flow field.

Figures 5 and 6 show the effect of the local Biot number Bi the process of convective heating increases on the thermal and species concentration in the boundary layers respectively for both cylinder and plate. For Biot number smaller than 0.1 the heat conduction inside the body is quicker than the heat convection away from its surface, and temperature gradients are negligible inside of it. Having a Biot number smaller than 0.1 labels a substance as thermally thin, and temperature can be assumed to be constant throughout the materials volume. The opposite is also true: A Biot number greater than 0.1 (a “thermally thick” substance) indicates that one cannot make this assumption, and more complicated heat transfer equations for “transient heat conduction” will be required to describe the time-varying and non-spatially-uniform temperature field within the material body. Physically, a large Biot number simulates a strong surface convection which as a result provides more heat to the surface of the sheet. More over concentration boundary layer thickness decreases with the strong convective heating.

An increase in Prandtl number Pr shows a decrease in temperature and thermal boundary layer thickness (see Fig. 7) for both cylinder and plate. Prandtl number is inversely proportional to the thermal diffusivity of fluid. Thermal diffusivity is weaker for higher Prandtl fluids and stronger for lower Prandtl fluids. Weaker thermal diffusivity corresponds to lower temperature and stronger thermal diffusivity shows higher temperature.

It is clearly observed that the concentration profiles increases at all points in the flow field with the increasing values of Soret number (Sr) this is shown in figure 8. This is because of the fact that the diffusive species with higher values of Soret parameter (Sr) has the tendency of increasing concentration profiles. Thus, it is concluded from Fig. 8 that the concentration distributions are more influenced with the values of Soret parameter. Figure 9 indicates that concentration is reduced continuously throughout the boundary-layer with increasing the value of Sc . Schmidt number measures the relative effectiveness of momentum and mass transport by diffusion. Larger values of Sc are equivalent to reducing the chemical molecular diffusivity i.e. less diffusion therefore takes place by mass transport.

Figure 10 is prepared to show the variation of skin friction factor with magnetic parameter and with different values of curvature parameter. It is noticed that the skin friction monotonically increases with curvature parameter and the same variation of skin friction factor can be observed for magnetic parameter at the boundary. The variation of the Nusselt number is shown for different parameters in Fig. 11. Figure 11 exhibit the behavior of heat transfer rates against Biot number and magnetic parameter with varies values of curvature parameter. The heat transfer rates diminish with an increase in magnetic parameter. Also it is noticed that the heat transfer rate for cylinder is higher as compared to plate surface. Bi arises in the wall temperature gradient boundary condition in Eq. (19). As Bi increases from $Bi = 0.1$ (thermally thin case) to $Bi > 0.1$ (thermally thick case) the rate of thermal conduction heat transfer inside the plate becomes dramatically lower than the heat convection away from its surface, and temperature gradients are increased at the plate. Figure 12 shows the various values of magnetic parameter and Soret number with different values of curvature parameter against local Sherwood number. It is clear that magnetic field strength and Soret number reduces the local Sherwood number because concentration boundary layer thickness increases. Moreover local Sherwood number increases with a increase in curvature parameter.

V. CONCLUSIONS

In the present work, the MHD boundary layer flow and heat transfer over permeable stretching cylinder with thermo diffusion under convective heating have been investigated. The present results are in fine concurrence with those reported in open literature for some special cases. From the study, the following remarks can be summarized.

- On rising the magnetic parameter, the resultant dimensionless velocity distribution reduces within the boundary layer but the dimensionless temperature distribution increases within the boundary layer.
- The local skin friction coefficient decreases and local Nusselt number increases by increasing the magnetic parameter.
- Convective heating are strongly influenced the temperature and heat transfer rate in the boundary layer of the flow.

- On increasing the Soret number is to reduce the local Sherwood number but its boundary layer thickness increases.

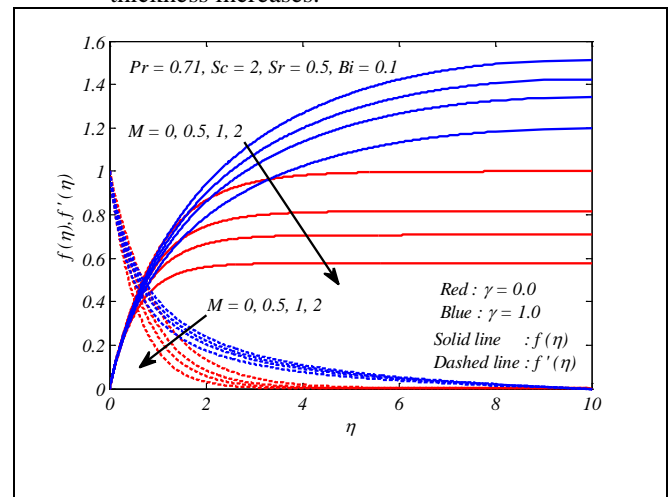


Figure 2: Dimensionless velocity distributions $f(\eta)$ & $f'(\eta)$ for different values of M .

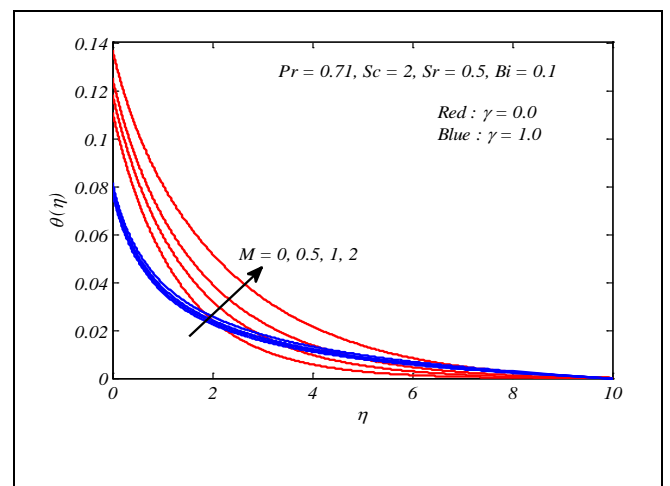


Figure 3: Dimensionless temperature distribution for different values of M .

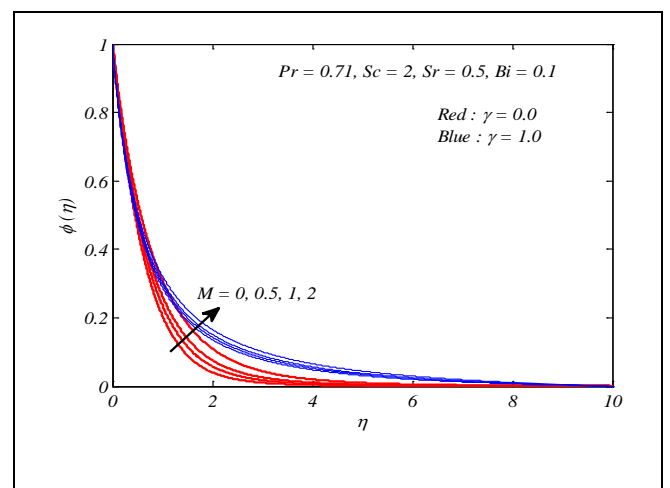


Figure 4: Concentration distribution for different values of M .

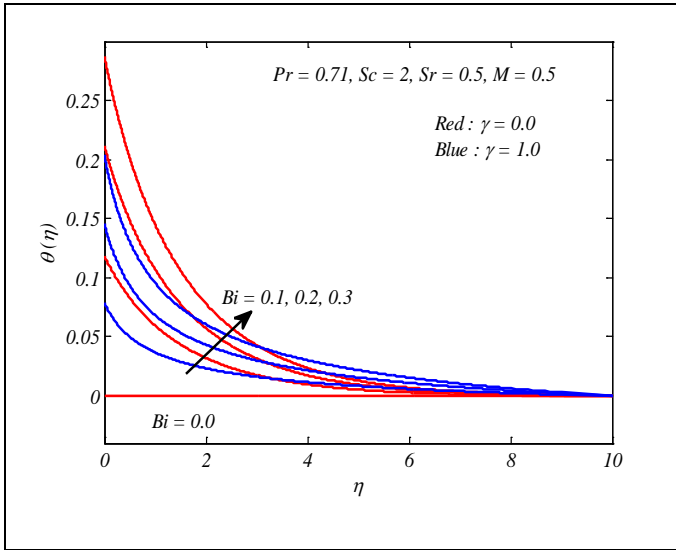


Figure 5: Dimensionless temperature distribution for different values of Bi .

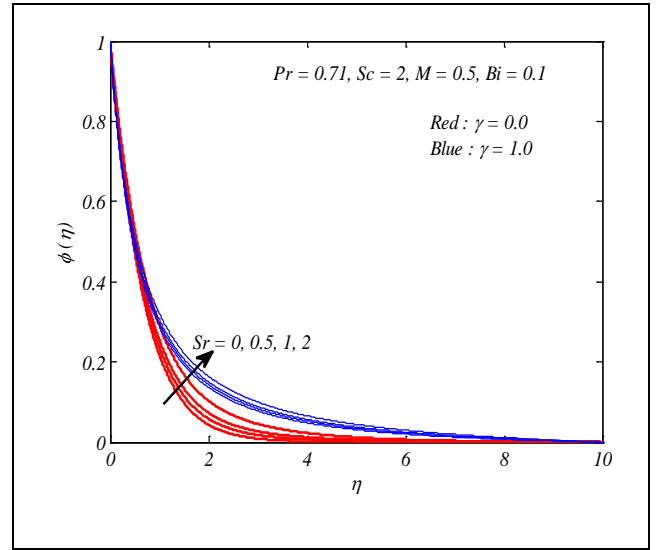


Figure 8: Dimensionless concentration distribution for different values of Sr .

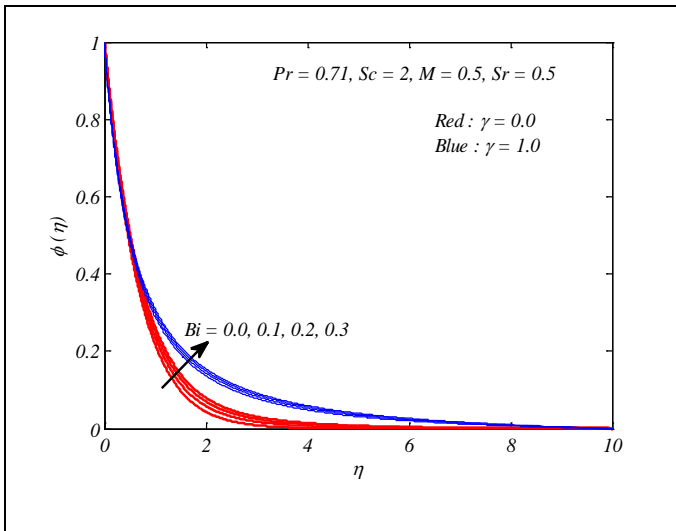


Figure 6: Dimensionless concentration distribution for different values of Bi .

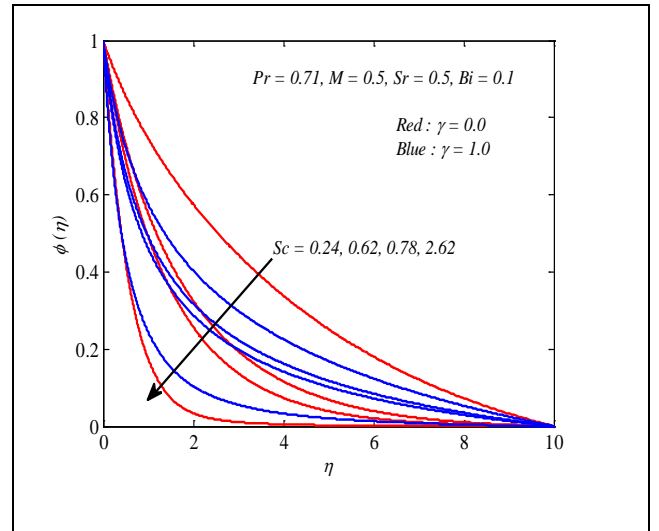


Figure 9: Dimensionless concentration distribution for different values of Sc .

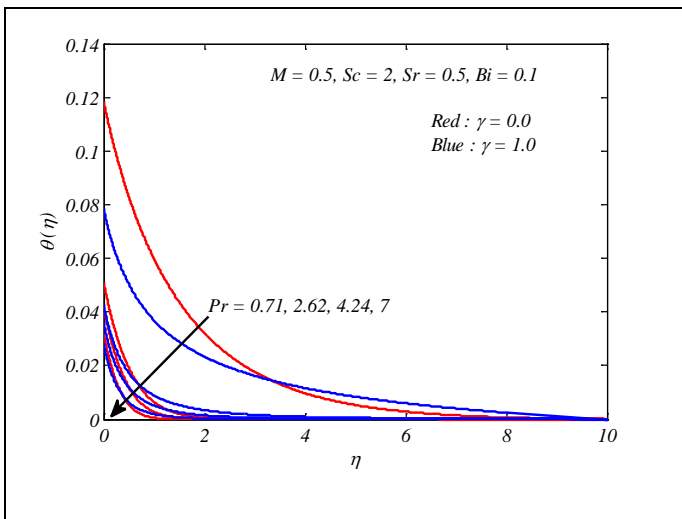


Figure 7: Dimensionless temperature distribution for different values of Pr .

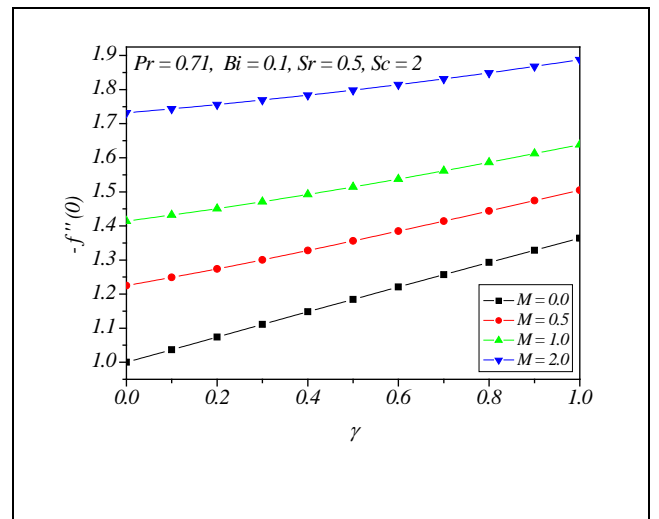


Figure 10: Skin friction coefficient for different values of M and γ .

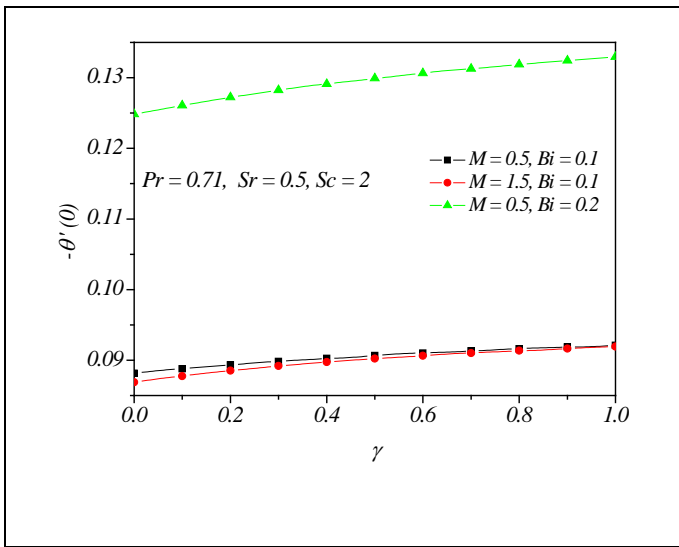


Figure 11: Local Nusselt number for different values of M , Bi and γ .

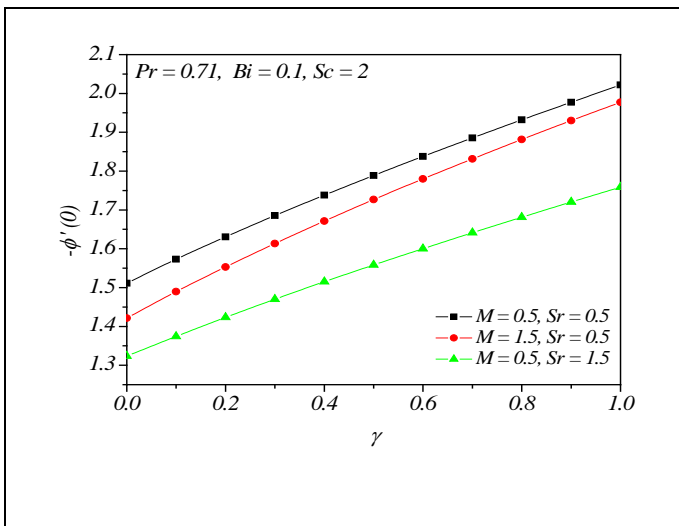


Figure 12: Local Sherwood number for different values of M , Sr and γ .

Table 1: Comparison of skin friction coefficient for different values of M when $\gamma = 0$.

| M | Butt and Ali [20] | Fang et al. [21] | Mukhopadhyay [22] | Maboob et al. [23] | Present results |
|------|-------------------|------------------|-------------------|--------------------|-----------------|
| 0.25 | - | 1.1180 | 1.1180 | 1.1180 | 1.118035 |
| 1 | - | - | 1.4142 | 1.4142 | 1.414214 |
| 2.25 | - | - | 1.8027 | 1.8027 | 1.802776 |
| 4 | - | 2.2361 | 2.2361 | 2.2361 | 2.236063 |

VI.

VII. REFERENCES

[1] Rehman A, Nadeem S., (2012), Mixed convection heat transfer in micropolar nanofluid over a vertical slender cylinder, Chin Phys Lett., Vol. 29(12), pp.124701.

[2] Olanrewaju, P. O., Okedayo, G. T., Gbadeyan, J. A., (2011), Effects of thermal radiation on magneto hydro dynamic (MHD) flow of a micro polar fluid towards a stagnation point on a vertical place, Int.J. Of App.Sci. and Tech., Vol.1 No.6, pp.219-230.

[3] Gangadhar, K., (2012), Radiation and viscous Dissipation effects on chemically reacting MHD boundary layer flow of heat and mass transfer through a porous vertical flat plate. Journal of Energy, Heat and Mass Transfer, Vol. 34, pp.245-259.

[4] Mohammed Ibrahim. S., Gangadhar, K., and Bhaskar Reddy, N., (2015), Radiation and Mass Transfer Effects on MHD Oscillatory Flow in a Channel Filled with Porous Medium in the presence of Chemical Reaction, Journal of Applied Fluid Mechanics, Vol.8, No.3, pp.529-537.

[5] Rawat, S., Kapoor, S., and Bhargava, R., (2016), MHD Flow and heat and Mass Transfer of Micropolar Fluid over a Nonlinear Stretching Sheet with Variable Micro Inertia Density, Heat Flux and Chemical Reaction in a Non-Darcy Porous Medium, Journal of Applied Fluid Mechanics, Vol.9, No.1, pp.321-331.

[6] E. R. G. Eckert and R. M. Drake, Analysis of Heat and Mass Transfer. McGraw-Hill, New York, 1972.

[7] O. D. Makinde, P. O. Olanrewaju: Unsteady mixed convection with Soret and Dufour effects past a porous plate moving through a binary mixture of chemically reacting fluid. Chemical Engineering Communications, 198 (7), 920-938, 2011.

[8] S. A. Shehzad, F. E. Alsaadi, S. J. Monaquel and T. Hayat, Soret and Dufour effects on the stagnation point flow of Jeffery fluid with convective boundary conditions, Eur. Phys. J. Plus, 128, (2013) 56.

[9] O. D. Makinde: On MHD mixed convection with Soret and Dufour effects past a vertical plate embedded in a porous medium. Latin American Applied Research, 41, 63-68, 2011.

[10] P. O. Olanrewaju and O. D. Makinde: Effects of thermal diffusion and diffusion thermo on chemically reacting MHD boundary layer flow of heat and mass transfer past a moving vertical plate with suction/injection. Arabian Journal of Science and Engineering, 36, 1607-1619, 2011.

[11] Aziz A, (2009), A similarity solution for laminar thermal boundary layer over a flat plate with a convective surface boundary condition, Commun. Nonlinear Sci. Numer. Simulat, Vol.14, pp.1064-1068.

[12] Bataller RC, (2008), Radiation effects for the Blasius and Sakiadis flows with a convective surface boundary condition, Appl. Math. Comput., Vol.206, pp.832-840.

[13] Gangadhar K, Bhaskar Reddy N, Kameswaran PK, (2012), Similarity Solution of Hydro-Magnetic Heat and Mass Transfer over a Vertical Plate with a Convective Surface Boundary Condition and Chemical Reaction, International Journal of Nonlinear Science, Vol.13(3), pp-298-307.

[14] Ishak A, (2010), Similarity solutions for flow and heat transfer over a permeable surface with convective boundary condition, Appl. Math. Computation, Vol.217, pp.837-842.

[15] Makinde OD and Aziz A, (2011), Boundary layer flow of a nanofluid past a stretching sheet with a convective boundary condition, Int. J. Therm. Sci., Vol.50, pp.1326-1332.

[16] Mukhopadhyay S, (2013), MHD boundary layer slip flow along a stretching cylinder, Ain Shams Eng. J., Vol. 4, pp.317-324.

[17] Bachok N, Ishak A, (2010), Flow and heat transfer over a stretching cylinder with prescribed surface heat flux, Malays. J. Math. Sci., Vol.4, pp.159-169.

- [18] Ishak A, Nazar R, Arifin NM, Ali FM, Pop I, (2011), MHD stagnation-point flow towards a stretching sheet with prescribed surface heat flux, Sains Malays., Vol.40, pp.1193–1199.
- [19] Liu IC, (2005), A note on heat and mass transfer for a hydromagnetics flow over a stretching sheet, Int. Commun. Heat Mass Transf., Vol. 32, pp.1075–1084.
- [20] Butt AS, Ali A, (2014), Computational study of entropy generation in magnetohydrodynamic flow and heat transfer over an unsteady stretching permeable sheet, Eur. Phys. J. Plus, Vol.129, pp.13.
- [21] Fang T, Zhang J, Yao S, (2009), Slip MHD viscous flow over a stretching sheet-an exact solution, Commun. Nonlinear Sci. Numer. Simul., Vol. 14, pp.3731–3737.
- [22] Mukhopadhyay S, (2011), Chemically reactive solute transfer in a boundary layer slip flow along a stretching cylinder, Front. Chem. Sci. Eng., Vol. 5, pp.385–391.
- [23] Mabood F, Lorenzini G, Pochai N, Muhammad Ibrahim S, (2016), Effects of prescribed heat flux and transpiration on MHD axisymmetric flow impinging on stretching cylinder, Continuum Mech. Thermodyn., DOI 10.1007/s00161-016-0519-9.